Appl. Phys. B 72, 839–842 (2001) / Digital Object Identifier (DOI) 10.1007/s003400100575

Applied Physics B
Lasers
and Optics

The optimum configuration for the third-harmonic generation of 1.064 μm in a YCOB crystal

Z. Wang*, K. Fu, X. Xu, X. Sun, H. Jiang, R. Song, J. Liu, J. Wang, Y. Liu, J. Wei, Z. Shao

State Key Laboratory of Crystal Materials, Shandong University, Ji'nan 250100, Shandong, P.R. China

Received: 11 September 2000/Revised version: 25 January 2001/Published online: 27 April 2001 –

Abstract. A method of determining the spatial configuration of a $YCa_4O(BO_3)_3$ (YCOB) crystal is introduced. The type-I phase-matching points for the sum-frequency of 1.064 μm and 0.532 μm, as well as the conversion efficiency for YCOB samples cut in different directions, have been measured. When the input intensity is 0.76 GW/cm^2, the third-harmonic generation (THG) conversion efficiency for the (106°, 77.2°)-cut YCOB crystal reaches 26.2%, which is the highest that we know so far. Both the calculations and the experiments show that the optimum THG configuration for a YCOB crystal is near (106°, 77.2°), or other equivalent directions in space.

PACS: 42.65.Ky; 42.70.Mp

Recently, visible and UV lasers have been in great demand for many applications, e.g. laser processing, optical data storage, and medical treatment. To obtain such lasers, frequency conversion of solid-state lasers by using a non-linear optical (NLO) crystal is an efficient method. Nowadays the most widely used NLO crystal for second-harmonic generation is KTP ($KTiOPO_4$). For UV laser-beam generation, LBO (LiB_3O_5) and β-BBO (β-BaB_2O_4) play the main roles, but the difficulty of growth and hygroscopicity have limited their applications.

During the last few years, there has been great interest in the new NLO material of $ReCa_4O(BO_3)_3$ (ReCOB) (Re = Y, Gd). In 1997, Aka et al. reported the linear- and non-linear-optical properties of GdCOB [1]. Later, Iwai et al. introduced the growth of YCOB and GdCOB, as well as some optical characterizations, including the transmission, refractive indices, and frequency-doubling property [2].

Since these two crystals melt congruently, they can be grown rapidly by the Czochralski method, and it is easy to get a large crystal with high optical quality. Other famous non-linear crystals, such as KDP, KTP, LBO, and β-BBO, do not possess this advantage. The laser damage threshold of GdCOB reaches 1 GW/cm^2 when the incident pulse is 7-ns long at 532 nm, which is similar to that of BBO [1]. Furthermore, ReCOB has other attractive properties such as wide transmission band, large phase-matching range, non-hygroscopicity, and good mechanical properties, which allow easy polishing. All these properties make ReCOB a promising crystal in the frequency-conversion domain.

From the Sellmeier equations of YCOB and GdCOB crystals [1, 2], we know that YCOB can reach type-I phase matching for the sum-frequency of 1.064 μm and 0.532 μm, while GdCOB can not. Another advantage of YCOB is that the transmission limit can be as short as 200 nm, while for GdCOB there are several sharp absorption peaks in the region of 200–320 nm. In this way it can be said that a YCOB crystal is more suitable for UV laser-beam generation. In 1999, Yoshimura et al. reported the third-harmonic generation of 1064 nm in a YCOB crystal cut in the XY principal plane, and the THG conversion efficiency was about 2.5% [3]. In a previous work, we have improved this value to 9.8% by a 7-mm-long, (90°, 73.8°)-cut YCOB crystal [4]. Because YCOB belongs to a low symmetric monoclinic crystal system, its maximum d_{eff} (effective non-linear coefficient) is not in the principal planes, but in a general spatial direction. Searching for this direction is helpful to get a higher THG conversion efficiency, and the potential in this application of the crystal will be explored effectively. According to the second-order non-linear-optical susceptibilities of YCOB, we have fitted the spatial distribution curve of d_{eff} for the THG of 1064 nm. This distribution rule is proved by the following experiments on four YCOB samples. When the input intensity is 0.76 GW/cm^2, the THG conversion efficiency of (106°, 77.2°)-cut YCOB reaches 26.2%, which is the best result that we know so far. Though Yoshimura et al. have achieved the non-critical THG phase matching of 1064 nm with a $Gd_xY_{1-x}COB$ ($x = 0.24$) crystal, the THG conversion efficiency is no more than 15% [3]. Furthermore, we have found the mixing parameter x will be quite different when the growth conditions change. When x is in the range of $0.2 - 0.8$, the quality of $Gd_xY_{1-x}COB$ is harder to guarantee, as compared with pure YCOB or GdCOB. A detailed discussion on $Gd_xY_{1-x}COB$ will be reported in another paper. Above all, we have proved that the optimum THG

*Corresponding author.
Postal address: Institute of Crystal Materials, Shandong University, Ji'nan 250100, Shandong, P.R. China.
(Fax: +86-531/856-5403, E-mail: zshao@icm.sdu.edu.cn)

direction of YCOB is near (106°, 77.2°), or other equivalent directions in space.

1 Determination of spatial configuration

For NLO crystals, the magnitude of d_{eff} has a crucial influence on the frequency-conversion process. YCOB has the point group m and the space group C_m. The symmetry of d_{eff} is $2/m$, and two independent quadrants are needed to determine its complete distribution. In the processing course of YCOB, the method of how to confirm the spatial direction is very important.

In this paper we use polar coordinates to define the spatial direction, which coincides with the usual convention. Each direction $\boldsymbol{K}$ is expressed in the form of (θ, ϕ), where θ is the polar angle and ϕ is the azimuthal angle. This definition is shown in Fig. 1, where X, Y, Z are the main refractive-index axes observing the rule $n_X < n_Y < n_Z$. For monoclinic biaxial crystals such as YCOB, the main refractive axes (X, Y, Z) do not correspond to the crystallographic axes (a, b, c). The orientation relationship has been reported by Ye and Chai [5], and here we show it in Fig. 1.

Three reference planes are needed for the determination of a spatial configuration, and it is necessary especially for the low-symmetric crystals. For YCOB we chose (010), $(\bar{2}01)$, (202) as our reference planes. With the unit-cell constants of a YCOB crystal reported by Iwai et al. [2], the angle between the (202) plane and the X-axis is calculated to be 45°, so the angle between $\boldsymbol{N}$ and the X-axis is 45°, where $\boldsymbol{N}$ is the normal direction of the (202) plane. In the orthogonal reference frame decided by X, Y, and Z, the directional cosines of vector $\boldsymbol{N}$ are $(\cos 45°, 0, \sin 45°)$ and the directional cosines of vector $\boldsymbol{K}(\theta, \phi)$ are $(\sin\theta\cos\phi, \sin\theta\sin\phi, \cos\theta)$. From knowledge of analytic geometry, the angle between $\boldsymbol{N}$ and $\boldsymbol{K}$ is

$$\Psi_1 = \arccos(\cos 45° \sin\theta\cos\phi + \sin 45° \cos\theta) \quad (1)$$

as shown in Fig. 1. According to the same principle, the other two angles are

$$\Psi_2 = \arccos(\cos 25° \sin\theta\cos\phi - \sin 25° \cos\theta) \quad (2)$$

$$\Psi_3 = \arccos(-\sin\theta\sin\phi)\,, \quad (3)$$

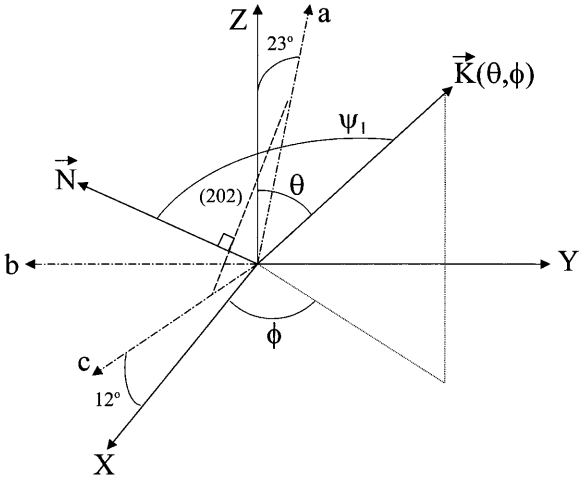

Fig. 1. Reference diagram for the processing of YCOB crystal

where Ψ_2 is the angle between the normal direction of the $(\bar{2}01)$ plane and $\boldsymbol{K}$, and Ψ_3 is the angle between the normal direction of the (010) plane and $\boldsymbol{K}$. The angles between the transparent plane (perpendicular to $\boldsymbol{K}$) and reference planes are used in the processing procedure, and they are supplementary angles of Ψ_1, Ψ_2, and Ψ_3. By these relationships, we can process crystal samples cut in any spatial direction. For other NLO crystals, not all the three reference planes are needed because they are attributed to a higher symmetric system, and it makes the processing course easier than that of YCOB.

2 Measurement of THG phase-matching angle

The experimental setup is shown in Fig. 2. The fundamental light is provided by a PY61 Nd:YAG picosecond laser, which was manufactured by the Continuum Corp., USA. Its working wavelength is 1064 nm, the repeat frequency is 10 Hz, and the pulse width is 35 ps. To improve the quality of the input light, a diaphragm ($\phi = 2.5$ mm) is set before the crystal sample. A filter ($T = 73\%$ at 355 nm, $T < 1\%$ at 1064 nm, 532 nm) is placed between the crystal and the energy meter to block the first- and the second-harmonic laser beams. A 5-mm-long KTP crystal is used to generate the doubling frequency of 1064 nm. The dimensions of the YCOB crystal used in this experiment are $20 \times 7 \times 15$ mm^3. The Y plane is polished, but uncoated. The X and Z planes are processed to be side planes, respectively. This crystal is mounted on a Fedorow table that can be adjusted to any direction in space.

The measured phase matching (PM) points are shown in Fig. 3. The PM point in the XY plane is (90°, 73.8°), and in the YZ plane is (59.8°, 90°). These points are fitted to curve a, as shown in Fig. 3. Based on the two sets of Sellmeier equations published before [2, 6], we calculate the PM curves for

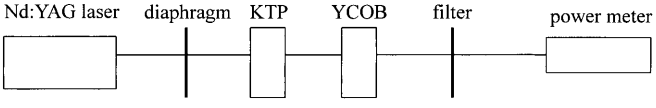

Fig. 2. Experimental setup for the measurement of the phase matching points and the sum-frequency conversion-efficiency

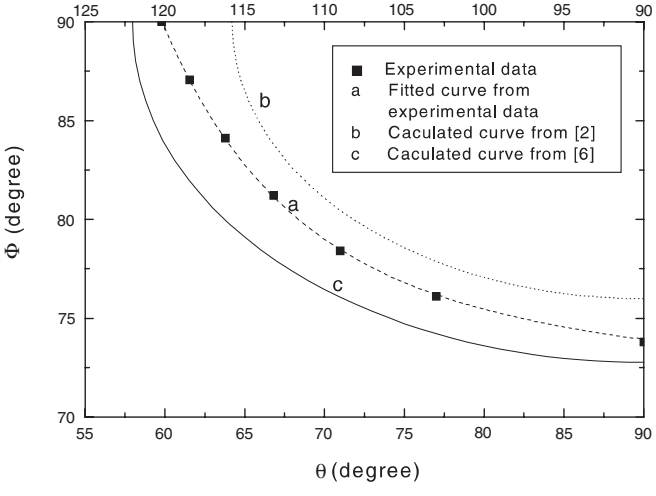

Fig. 3. Type-I phase-matching curves for THG of 1064 nm in YCOB

a type-I sum-frequency of 1064 nm + 532 nm → 355 nm in YCOB, as b and c in Fig. 3. The experimental curve is located between the two calculated curves, indicating that the practical index in the ultraviolet region has some discrepancy with both the two Sellmeier equations.

3 The spatial distribution of effective non-linear coefficient

As far as the Kleimann symmetry is concerned, the contracted matrix of non-linear coefficients $[d_{in}]$ can be expressed as follows:

$$\begin{pmatrix} d_{11} & d_{12} & d_{13} & 0 & d_{31} & 0 \\ 0 & 0 & 0 & d_{32} & 0 & d_{12} \\ d_{31} & d_{32} & d_{33} & 0 & d_{13} & 0 \end{pmatrix}. \quad (4)$$

Scaling all these non-linear coefficients is complicated work. In Chen et al. [7], they have been determined as follows: $d_{11} = 0.056\,\text{pm/V}$, $d_{12} = 0.128\,\text{pm/V}$, $d_{13} = -0.186\,\text{pm/V}$, $d_{31} = 0.151\,\text{pm/V}$, $d_{32} = 1.36\,\text{pm/V}$, $d_{33} = -0.93\,\text{pm/V}$, where $d_{11}, d_{12}, d_{13}, d_{31}$ are theoretical values calculated from complete neglect of differential overlap (CNDO) programs, and d_{32}, d_{33} are experimental values obtained from the Maker Fringes measurement. The signs of d_{32}, d_{33} are determined from CNDO programs. A further calculation indicates that the largest d_{eff} for second-harmonic generation (SHG) in YCOB is in the region of $(90° < \theta < 180°, 0° < \phi < 90°)$, which has been proved by experiments. By the PM SHG method, Mougel et al. [6] have also measured some non-linear coefficients, i.e. d_{12}, d_{31}, and d_{32}. Their results appear larger than those reported by Chen et al. The origin of this discrepancy may come from the use of different methods. To clarify this, further theoretical and experimental research work needs to be performed.

Because the d_{ij} data reported by Chen et al. are more integrated, and the SHG property speculated from them has been proved successfully, here we use them in the following calculation. Associating them with the two sets of Sellmeier equations [2, 6], we fit the spatial distributions of $|d_{\text{eff}}|$ for THG in YCOB, as shown in Fig. 4. The non-linear coefficients we used are determined by SHG experiments, and in fact the magnitude of them depends on the wavelengths of the interacting waves; so the calculated results may be somewhat different from the actual situation. Nevertheless, the varying trend of d_{eff} is considered to be reliable. Both curves exhibit that the maximum d_{eff} is not in the principal planes or the first quadrant $(90° > \theta > 0°, 90° > \phi > 0°)$, but in the second quadrant $(180° > \theta > 90°, 90° > \phi > 0°)$. d_{eff} in the XY plane is larger than that in the YZ plane, which has been proved by our prior experiment [4].

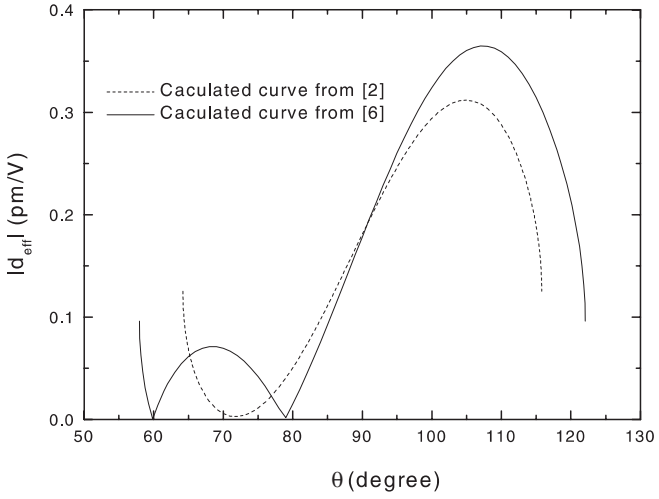

Fig. 4. The distribution of $|d_{\text{eff}}|$ for the THG of 1064 μm in YCOB

4 THG experiments on different YCOB samples

From curve a in Fig. 3, we choose four points to process the crystal samples, which are (65°, 82.8°), (90°, 73.8°), (106°, 77.2°), and (111°, 79.6°). All these crystals are 10.4 mm in length, and their transmission ends are polished. The experimental setup has been shown in Fig. 2. The THG output is measured, and the results are shown in Figs. 5 and 6. From these figures we know that (106°, 77.2°)-cut YCOB has the largest THG output. When the input intensity is $0.76\,\text{GW/cm}^2$, its THG conversion efficiency reaches 26.2%. As far as we know, it is the best result for a YCOB crystal reported to date. For the (111°, 79.6°)-cut YCOB and the (90°, 73.8°)-cut YCOB,

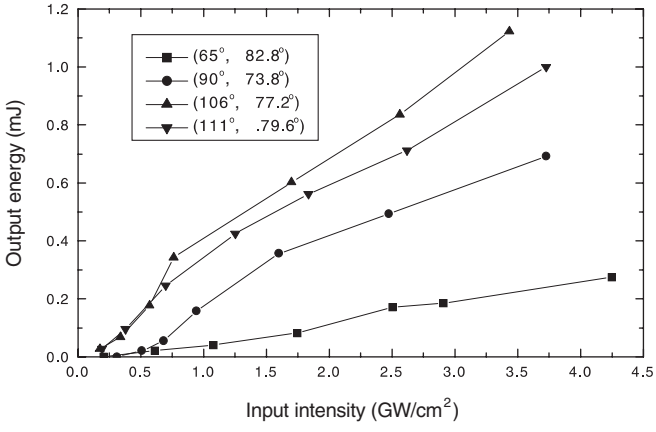

Fig. 5. The THG output energy vs. input intensity

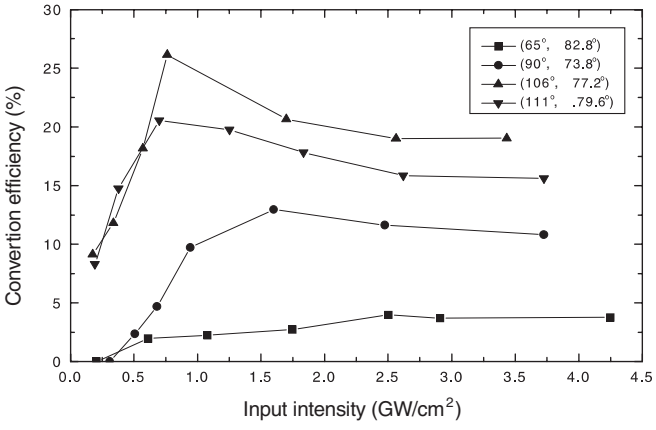

Fig. 6. The THG convertion efficiency vs. input intensity

the conversion efficiency is lower. For the (65°, 82.8°)-cut YCOB, the conversion efficiency is the lowest (< 5%). Generally, the THG output of these crystals is consistent with the distribution rules shown in Fig. 4. Both the experiments and the calculations have shown that the maximum d_{eff} is near the direction of (106°, 77.2°), or other equivalent regions. When the input intensity is larger than $1\,\text{GW/cm}^2$, the THG conversion efficiency decreases gradually. The explanation of this phenomenon can be found in the literature [8–11].

5 Conclusion

In this paper we report research on the sum-frequency for $1.064\,\mu\text{m} + 0.532\,\mu\text{m} \rightarrow 0.355\,\mu\text{m}$ in a YCOB crystal. The type-I PM points, as well as the THG conversion efficiency of different YCOB samples, have been measured. When the PM angle is $\theta = 106°$, $\phi = 77.2°$, the THG conversion efficiency reaches 26.2% under the input intensity of $0.76\,\text{GW/cm}^2$, which is the best result for a YCOB crystal reported so far. Our experiments and calculations have shown that the maximum d_{eff} for this sum-frequency is near the direction of (106°, 77.2°) in the second quadrant, or its equivalent directions in other quadrants. We believe that our research result is helpful for the further research and the applications of YCOB crystals, as well as for other low-symmetric non-linear crystals.

Acknowledgements. This work was supported by the Key Program of National Natural Science Foundation of China under Grant No. 69890235, and the Research Award Foundation for Excellent Youth Scientists of Shandong Province of China.

References

1. G. Aka, A. Kahn-Harari, F. Mougel, D. Vivien, F. Salin, P. Coquelin, P. Colin, D. Pelenc, J.P. Damelet: J. Opt. Soc. Am. B **14**, 2238 (1997)
2. M. Iwai, T. Kobayashi, H. Furuya, Y. Mori, T. Sasaki: Jpn. J. Appl. Phys. **36**, L276 (1997)
3. M. Yoshimura, H. Furuya, I. Yamada, K. Murase, H. Nakao, M. Yamazaki, Y. Mori, T. Sasaki: CLEO'99, Tech. Dig., CFF2: 529, 530
4. Z. Wang, G. Zhou, C. Wang, R. Song, H. Jiang, K. Fu, C. Wang, J. Liu, J. Wang, Y. Liu, J. Wei, Z. Shao: J. Optoelectron. Laser **11**, 606 (2000) [in Chinese]
5. Q. Ye, B.H.T. Chai: J. Cryst. Growth **197**, 228 (1999)
6. F. Mougel, G. Aka, F. Salin, D. Pelenc, A. Kahn-Harari, D. Vivien: Accurate second-harmonic generation phase-matching angle prediction and non-linear coefficient measurements of $Ca_4YO(BO_3)_3$ (YCOB) crystal. 1999 Advanced Solid State Laser Meeting, Tech. Dig., WB11: 332–334
7. C. Chen, Z. Shao, J. Jiang, J. Wei, J. Lin, J. Wang, N. Ye, J. Lv, B. Wu, M. Jiang, M. Yoshimura, Y. Mori, T. Sasaki: J. Opt. Soc. Am. B. **17**, 566 (2000)
8. R.S. Craxton: IEEE J. Quantum Electron. **QE-17**, 1771 (1981)
9. X. Wei, W. Zheng: High Power Laser Part. Beams **11**, 11 (1999) [in Chinese]
10. C.Y. Chien, G. Korn, J.S. Coe, J. Squier, G. Mourou: Opt. Lett. **20**, 353 (1995)
11. X. Wei, X. Zhang, Z. Sui, X. Yuan: Chin. J. Lasers **17**, 737 (1990) [in Chinese]